*The Pharmaceutical and Chemical Journal*, 2020, 7(3):56-68

*Available online www.tpcj.org*

**Research Article**

**ISSN: 2349-7092**
**CODEN(USA): PCJHBA**

# Adsorption and Corrosion Inhibitive Properties of 1-Methyl-1*H*-imidazole-2-thiol on Mild Steel in Acidic Environment

**Omar Benali[1,2]*, Aïssa Benikdes[2,3], Driss Ben Hmamou[4]**

[1]Department of Biology, Faculty of Sciences, Dr Moulay Tahar University of Saïda, Algeria.
[2]Laboratory of Chemistry, Synthesis, Properties and Applications, Dr Moulay Tahar University of Saïda, Algeria.
[3]Department of Civil Engineering and Hydraulics, Faculty of Technology, Dr Moulay Tahar University of Saïda, Algeria.
[4]Laboratory of Applied Chemistry and Environment, ENSA, University Ibn Zohr, Agadir, Morocco.
*Corresponding author: benaliomar@hotmail.com

**Abstract** The inhibition effect of 1-methyl-1*H*-imidazole-2-thiol (MTI) on the corrosion of mild steel in 1 M HCl, 3M HCl, 0.5 M $H_2SO_4$ and 1.5 M $H_2SO_4$ solution was investigated electrochemical methods (potentiodynamic polarization curves, resistance polarization and electrochemical impedance spectroscopy). The results show that MTI is a very good inhibitor, and is more efficiency in 1 M HCl than the other medium. The ordere is 1 M HCl> 0.5 M $H_2SO_4$ >3M HCl > 1.5 M $H_2SO_4$. The adsorption of MTI on mild steel surface obeys Langmuir adsorption isotherm for 1 M HCl, 3M HCl and 0.5 M $H_2SO_4$, and El Awady kenetic-thermodynamic isotherm for 1.5 M $H_2SO_4$. Polarization curves reveal that MTI acts as a mixed-type inhibitor in both acids. The adsorption mechanism is discussed.

**Keywords** acid medium, mild steel, corrosion, inhibition

## 1. Introduction

Corrosion inhibition has been widely used for metal protection in aggressive environment. The use of the corrosion inhibitor was the most convenient and common way to improve the corrosion phenomenon [1-4]. Globally, organic compounds which containing nitrogen, oxygen, sulfur atoms and multiple bonds can be used as efficient inhibitors [5-8]. It was noticeable that imidazole and its derivatives had a wide application due to the advantages of high corrosion efficiency [9-13] and easy degradation [14]. The mechanism of such inhibitors had been interpreted as the adsorption process benefiting from the free electron pairs, the π-orbital character of free electrons and the electron density around the hetero-atoms [15-16]. On the other hand, imidazole is a planar, heterocyclic aromatic organic compound containing two nitrogen atoms that form a five-membered ring. One of the nitrogen atoms is pyrole type, and the other pyridine. The structure of imidazoles shows that these molecules have two sites suitable for linking to the surface: nitrogen atom with a free sp2 pair and the aromatic ring. Imidazoles are favourable as corrosion inhibitors due to the strong protective properties [17].

The aim of the present work was to investigate the possibility of mild steel protection from aggressive medium (1M HCl, 3M HCl, 0.5M $H_2SO_4$ and 1.5M $H_2SO_4$) by 1-methyl-1*H*-imidazole-2-thiol.

## 2. Experimental

1-methyl-1*H*-imidazole-2-thiol (Merck) was used as received. Fig. 1 shows the molecular structures of the investigated organic compound, which has been labeled **MIT.**

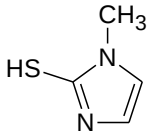


*Figure 1: Molecular structures of 1-methyl-1H-imidazole-2-thiol (MIT)*

The electrochemical study was carried out using a potentiostat PGZ100 piloted by Voltamaster software. This potentiostat is connected to a cell with three electrode thermostats with double wall (Tacussel Standard CEC/TH). A saturated calomel electrode (SCE) and platinum electrode were used as reference and auxiliary electrodes, respectively. The material used for constructing the working electrode having composition: 0.179% C, 0.165% Si, 0.439% Mn, 0.203% Cu, 0.034% S and Fe balance. Prior to all measurements, the exposed area was mechanically abraded with 180, 320, 800, 1200 grades of emery papers. The surface area exposed to the electrolyte is 0.04 $cm^2$.

Potentiodynamic polarization curves were plotted at a polarization scan rate of 0.5 mV/s. Before all experiments, the potential was stabilized at free potential during 30 min. The polarisation curves are obtained from −800 mV to −200 mV at 298 K. The solution test is there after de-aerated by bubbling nitrogen. Gas bubbling is maintained prior and through the experiments.

The polarization resistance measurements were performed by applying a controlled potential scan over a small range typically 10 mV with respect to $E_{corr}$. The resulting current is linearly plotted versus potential, the slope of this plot at E corr being the polarization resistance ($R_p$).

The electrochemical impedance spectroscopy (EIS) measurements are carried out with the same electrochemical system. After the determination of steady-state current at a corrosion potential, sine wave voltage (10 mV) peak to peak, at frequencies between 100 kHz and 10 mHz are superimposed on the rest potential. Computer programs automatically controlled the measurements performed at rest potentials after 0.5 hour of exposure at 298 K. The impedance diagrams are given in the Nyquist representation. Experiments are repeated three times to ensure the reproducibility.

Values of the charge transfer resistance $R_t$ were obtained from these plots by determining the difference in the values of impedance at low and high frequencies as suggested by Tsuru and Haruyama [18]. Values of the double−layer capacitance $C_{dl}$ were calculated from the frequency at which the impedance imaginary component $-Z_i$ is maximum using the equation:

$$f(-Zi_{max}) = \frac{1}{2\pi C_{dl} R_t} \quad (1)$$

The corrosion current densities were determined by Tafel extrapolation of the cathodic curves to the open circuit corrosion potentials.

The inhibition efficiency was evaluated from the measured $I_{corr}$ values using the relationship:

$$IE\ (\%) = I_{0corr} - I_{icorr}/I_{0corr} \times 100 \quad (2)$$

where $i_{0corr}$ and $i_{icorr}$ are the corrosion current density in absence and in presence of inhibitor, respectively.

The inhibition efficiency of the inhibitor has been found out from the polarization resistance values using the following equation:

$$IE\ (\%) = R_{ip} - R_{0p}/R_{ip} \times 100 \quad (3)$$

where $R_{0p}$ and $R_{ip}$ are the charge transfer resistance in absence and in presence of inhibitor, respectively.

The inhibition efficiency of the inhibitor has been found out from the charge transfer resistance values using the following equation:

$$IE\ (\%) = R_{it} - R_{0t}/R_{it} \times 100 \quad (4)$$

where $R_{0t}$ and $R_{it}$ are the charge transfer resistance in absence and in presence of inhibitor, respectively.

## 3. Results and Discussion

### 3.1. Polarization measurements

Potentiodynamic anodic and cathodic polarization scans were carried out at 298K with different concentrations of 1-methyl-1*H*-imidazole-2-thiol (**MIT**) in 1M HCl, 3M HCl, 0.5M $H_2SO_4$ and 1.5M $H_2SO_4$.

Anodic and cathodic polarization curves in the absence and in the presence of inhibitor at different concentrations after 30 min of immersion and at 298 K are shown in Figs. 2-5.

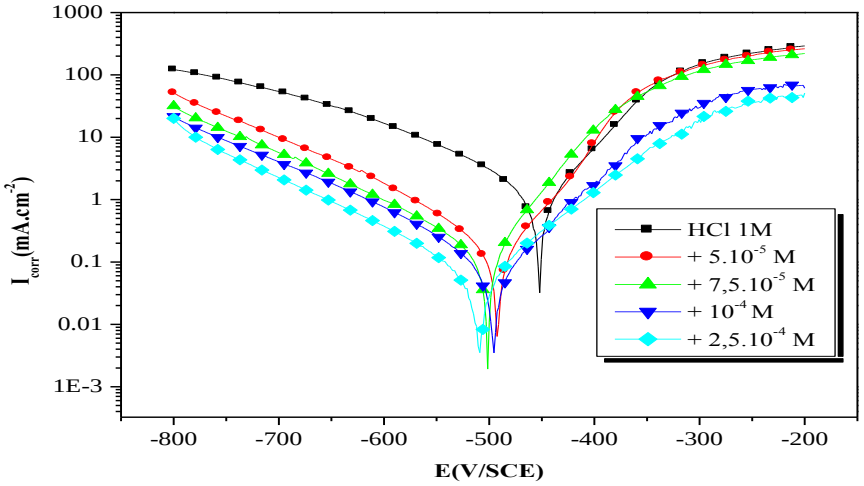


*Figure 2: Potentiodynamic polarization curves for mild steel in 1 M HCl containing different concentrations of MIT at 298 K*

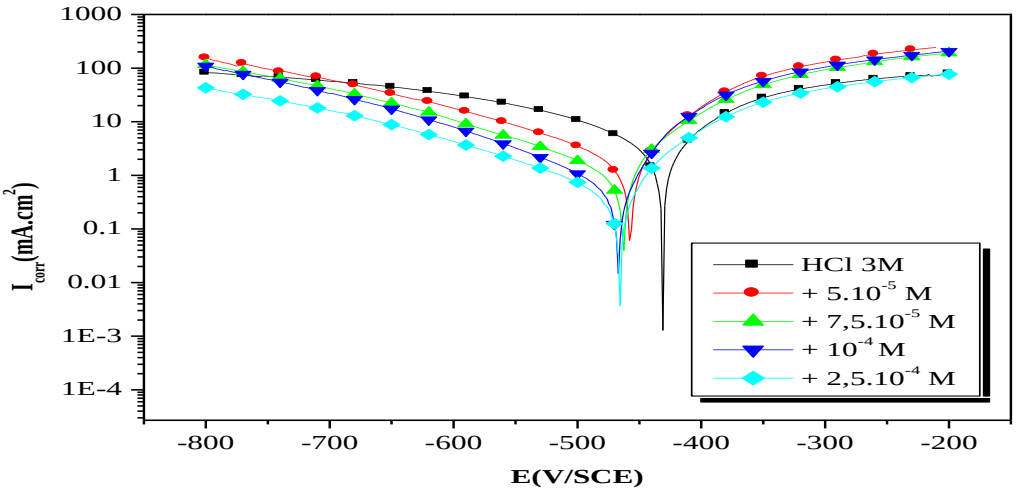


*Figure 3: Potentiodynamic polarization curves for mild steel in 1 M HCl containing different concentrations of MIT at 298 K*

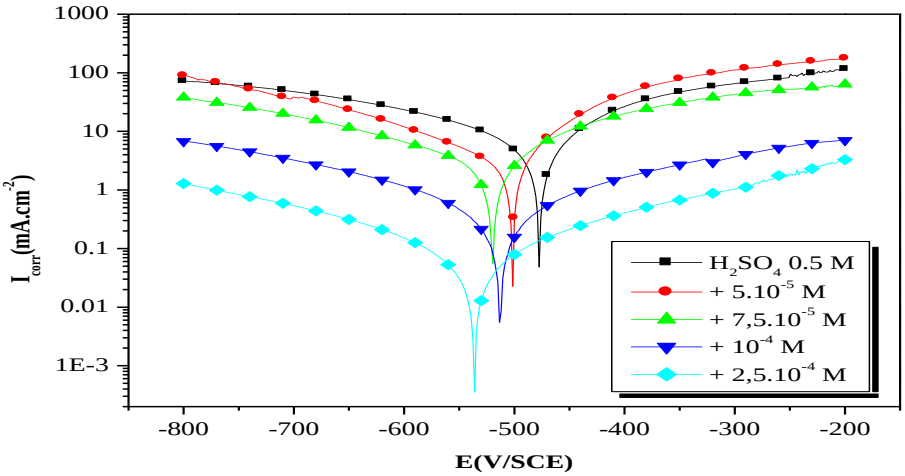


*Figure 4: Potentiodynamic polarization curves for mild steel in 0.5 M $H_2SO_4$ containing different concentrations of MIT at 298 K*

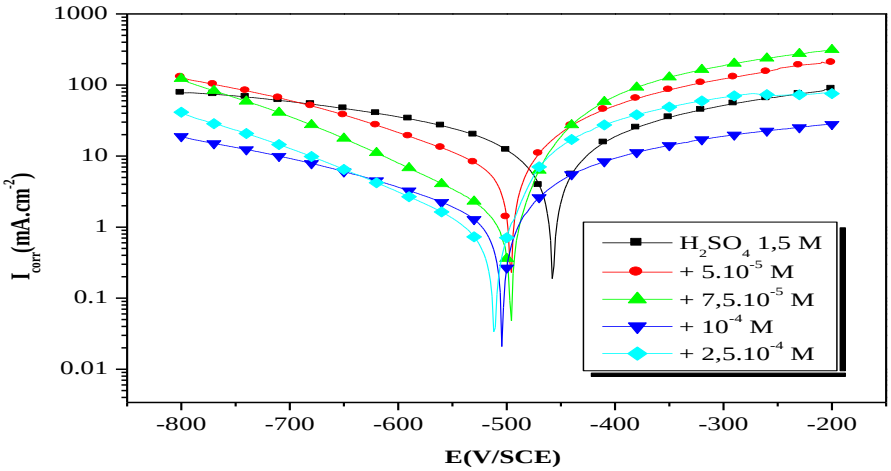


*Figure 5: Potentiodynamic polarization curves for mild steel in 0.5 M $H_2SO_4$ containing different concentrations of MIT at 298 K*

Analysis of these results makes it possible to raise more important points.

- The anodic and cathodic corrosion current ($I_{corr}$) values decrease with increasing concentration of inhibitor and in different acidic media.
- The cathodic polarization curves form quasi-parallel lines, this indicates that the introduction of the inhibitor to acid media does not modify the mechanism of the evolution of hydrogen and the reduction of $H^+$ ions on the surface of the metal instead mainly through a charge transfer mechanism. According to the literature, the cathodic reaction requires two successive stages [19]. The first is the discharge reaction (or Volmer reaction):

$$H^+_{ads} + e \rightarrow H_{ads}$$

The second step could be:

Or purely chemical: $H_{ads} + H_{ads} \rightarrow H_2$ (Tafel reaction)

Either electrochemical: $H_{ads} + H^+ + e \rightarrow H_2$ (Heyrovski reaction)

- In the case studied and according to the results in Table 1, the addition of the tested inhibitors causes a slight modification of the slopes of the Tafel lines ($\beta_c$). This result leads us to suggest that the proton reduction mechanism (the slowest) is not modified by the addition of inhibitors and that the latter follows the Heyroski model [19].
- A slight shift in corrosion potential ($E_{corr}$) should be noted. Under these conditions, an inhibitor is generally considered to be anodic or cathodic, when the difference between the corrosion potential ($E_{corr}$) without and with inhibitor is greater than 85 mv [20, 21]. In the present study, (Table 1) reveals a small shift in the corrosion potential of the order of 57 mV in maximum. In addition, the values of the corrosion potential ($E_{corr}$) shifted in the negative direction thus indicate that the inhibitor acts as a mixed inhibitor having a cathodic predominance.

**Table 1:** Electrochemical parameters and the corresponding corrosion inhibition efficiencies for the corrosion of mild steel in different medium containing MIT at 303 K

| | **Conc. (Mol/L)** | **$E_{corr}$ (mV/SCE)** | **$I_{corr}$ ($mA/cm^2$)** | **$-b_c$ (mV/dec)** | **$E_{Icorr}$ (%)** |
|---|---|---|---|---|---|
| HCl 1M | Blank | -452 | 2.66 | 165 | ----- |
| | $5 \times 10^{-5}$ | -492 | 0.41 | 137 | 84.54 |
| | $7.5 \times 10^{-5}$ | -501 | 0.24 | 121 | 90.82 |
| | $10^{-4}$ | -496 | 0.16 | 149 | 93.79 |
| | $2.5 \times 10^{-4}$ | -510 | 0.10 | 125 | 96.16 |
| HCl 3M | Blank | -430 | 12.61 | 165 | ----- |
| | $5 \times 10^{-5}$ | -456 | 6.49 | 151 | 48.53 |
| | $7.5 \times 10^{-5}$ | -462 | 3.75 | 164 | 70.26 |
| | $10^{-4}$ | -464 | 2.05 | 162 | 83.74 |
| | $2.5 \times 10^{-4}$ | -465 | 1.76 | 181 | 86.04 |
| $H_2SO_4$ 0.5M | Blank | -478 | 9.68 | 250 | --- |
| | $5 \times 10^{-5}$ | -502 | 4.64 | 213 | 52.06 |
| | $7.5 \times 10^{-5}$ | -519 | 2.43 | 207 | 74.89 |
| | $10^{-4}$ | -510 | 1.45 | 236 | 85.02 |
| | $2.5 \times 10^{-4}$ | -535 | 0.96 | 213 | 90.08 |
| $H_2SO_4$ 1.5M | Blank | -457 | 13.54 | 250 | --- |
| | $5 \times 10^{-5}$ | -496 | 11.35 | 251 | 16.17 |
| | $7.5 \times 10^{-5}$ | -496 | 6.35 | 187 | 53.10 |
| | $10^{-4}$ | -504 | 4.14 | 251 | 69.42 |
| | $2.5 \times 10^{-4}$ | -512 | 2.3 | 187 | 83.01 |

- From this analysis, it is very clear that the addition of the MIT decreases the speed of the two partial reactions by reducing the anodic dissolution and delaying the evolution of hydrogen reaction [16]. The addition of $5 \times 10^{-5}$M to $2.5 \times 10^{-4}$M of the inhibitor in question quickly leads to a decrease in the corrosion current density ($I_{corr}$) and an increase in the inhibition efficiency ($IE_{Icorr}$ %). The latter reaches the values of 96.16%; 90.08; 86.04% and 83.01 at $2.5 \times 10^{-4}$M in 1M HCl, 0.5M $H_2SO_4$, 3M HCl, and 1.5M $H_2SO_4$ respectively.
- Furthermore, we remark that when the lower concentrations in different medium, the anodic currents nearby the corrosion potential are higher than that measured in the blank solution. This can be explained as follows: it is known that the organic sulfur-containing compounds have two opposite effects on the corrosion of iron and steels. Firstly, they can chemisorb on the steel surface, segregate the metal surface from the solution and therefore inhibit the corrosion of iron and steels. Secondly, some of the organic

sulfur-containing compound molecules adsorbed on the surface of iron may decompose and give out $H_2S$, which can accelerate the corrosion of iron and steel in acid solutions [22]. Thus, when the concentration of MIT in 3M HCl is fairly low, the anodic dissolution of steel was accelerated by the $H_2S$ decomposed from MIT.

Linear polarization technique was performed in different medium with various concentrations of MIT. The corresponding polarization resistance ($R_p$) values of mild steel in the absence and in the presence of inhibitor concentrations are also given in Table 2. It is apparent that $R_p$ increases with increasing inhibitor concentration. The inhibition percentage ($IE_{Rp}$ %) calculated from $R_p$ values are also presented in Table 2. We remark that P% increases with increasing concentration of inhibitor and attains 94.14%; 84.15%; 83.84% and 85.47% at $2.5x10^{-4}$M in 1M HCl, 3M HCl, 0.5M $H_2SO_4$ and 1.5M $H_2SO_4$ respectively.

**Table 2.** Polarization resistance and the corresponding corrosion inhibition efficiencies for the corrosion of mild steel in different medium containing MIT at 303 K

| | **Conc. (Mol/L)** | **$R_p$ ($\Omega.cm^2$)** | **$IE_{Rp}$ (%)** |
|---|---|---|---|
| HCl 1 M | Blank | 11.96 | ----- |
| | $5 x10^{-5}$ | 60.71 | 80.29 |
| | $7.5 x10^{-5}$ | 79.18 | 84.89 |
| | $10^{-4}$ | 120,4 | 90.06 |
| | $2.5 x10^{-4}$ | 204.2 | 94.14 |
| HCl 3 M | Blank | 4.19 | ---- |
| | $5 x10^{-5}$ | 7.02 | 40.31 |
| | $7.5 x10^{-5}$ | 12.16 | 65.54 |
| | $10^{-4}$ | 17.62 | 76.22 |
| | $2.5 x10^{-4}$ | 26.45 | 84.15 |
| $H_2SO_4$ 0.5M | Blank | 2.62 | --- |
| | $5 x10^{-5}$ | 5.78 | 54.67 |
| | $7.5 x10^{-5}$ | 12.63 | 79.25 |
| | $10^{-4}$ | 14.11 | 81.43 |
| | $2.5 x10^{-4}$ | 16.22 | 83.84 |
| $H_2SO_4$ 1.5M | Blank | 1.30 | --- |
| | $5 x10^{-5}$ | 1.52 | 14.47 |
| | $7.5 x10^{-5}$ | 2.48 | 47.58 |
| | $10^{-4}$ | 4.28 | 69.62 |
| | $2.5 x10^{-4}$ | 8.95 | 85.47 |

**Electrochemical impedance spectroscopy**

With the aim of understanding the kinetics and characteristics of the electrochemical process on the mild steel surface in the acidic media and to get a better insight into the mechanism of corrosion inhibition, EIS measurements were performed. EIS is a non-destructive technique that is used for the rapid characterization and study of corrosion inhibition behavior. For mild steel, Nyquist plots obtained from EIS studies in the absence and presence of **MTI** at different concentration in 1M HCl, 3M HCl, 0.5M $H_2SO_4$ and 1.5M $H_2SO_4$ (after 30 min of immersion and at 298 K) are shown in Figs. 6-9.

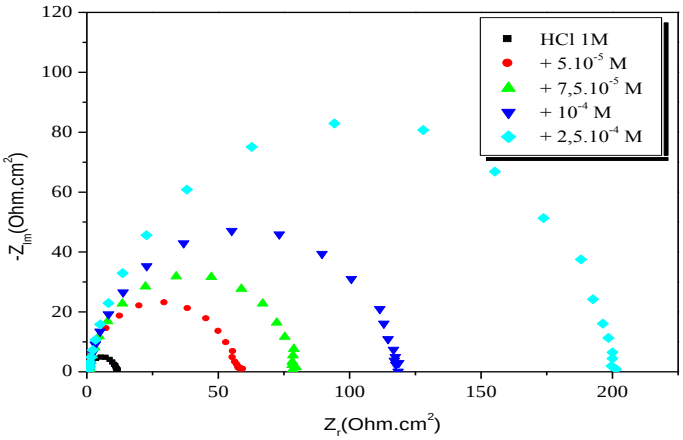


*Figure 6: Nyquist plots for mild steel in 1M HCl containing different concentrations of MTI*

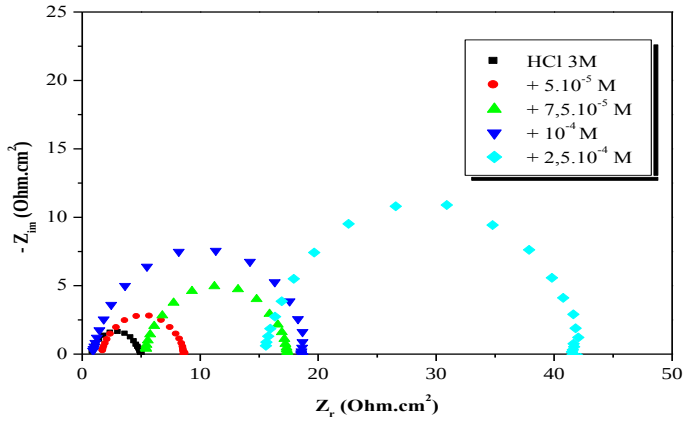


*Figure 7: Nyquist plots for mild steel in 3M HCl containing different concentrations of MTI*

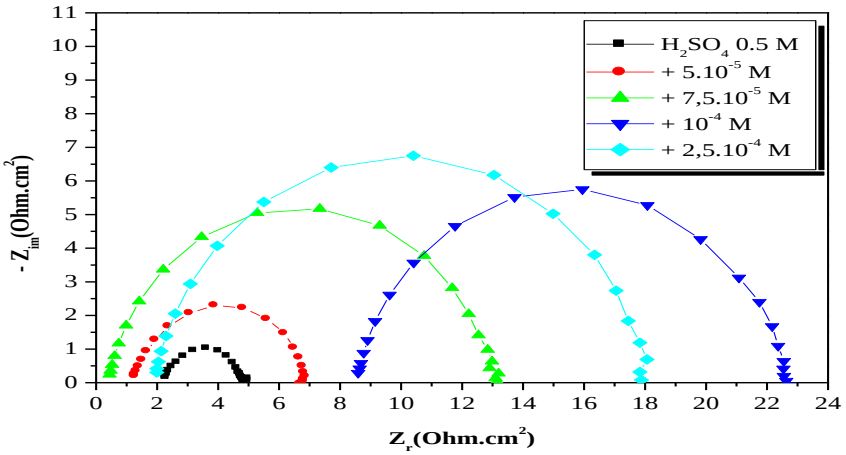


*Fig. 8. Nyquist plots for mild steel in 0.5M $H_2SO_4$ containing different concentrations of MTI*

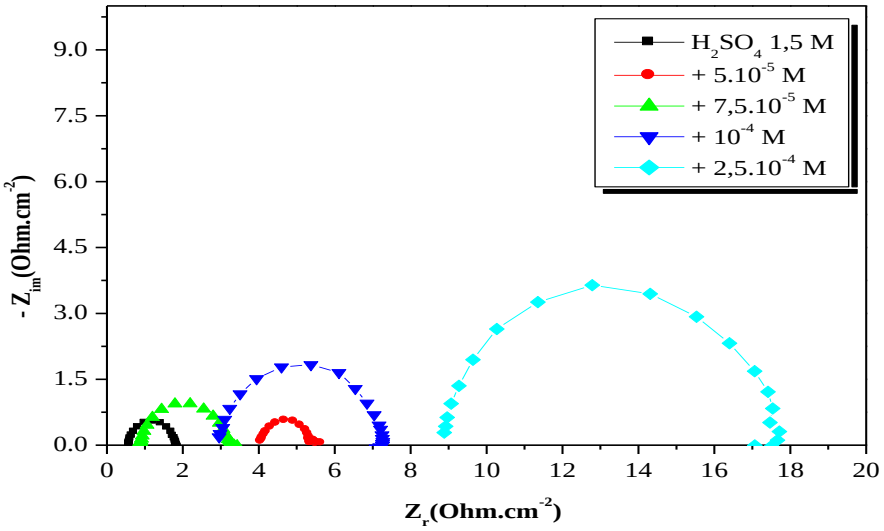


*Figure 9: Nyquist plots for mild steel in 0.5M $H_2SO_4$ containing different concentrations of MTI*

All the plots display a single capacitive loop. Impedance parameters derived from the Nyquist plots, percent inhibition efficiencies and the equivalent circuit diagram are given in Table 3 and Fig. 10, respectively.

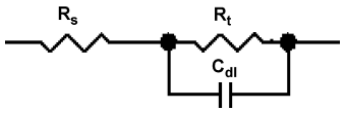


*Figure 10: The electrochemical equivalent circuit used to fit the impedance spectra*

**Table 3:** Impedance parameters and inhibition efficiency for the corrosion of mild steel in different medium containing different concentrations of **MTI**

| | Conc. (Mol/L) | $R_t$ ($\Omega.cm^2$) | $C_{dl}$ ($\mu F/cm^2$) | $IE_{Rt}$ (%) |
|---|---|---|---|---|
| HCl 1 M | Blank | 11.45 | 88.01 | ---- |
| | 5 x$10^{-5}$ | 57.99 | 68.64 | 80,25 |
| | 7.5 x$10^{-5}$ | 78.11 | 50.96 | 85.34 |
| | $10^{-4}$ | 118.9 | 49.60 | 90.37 |
| | 2.5 x$10^{-4}$ | 201.0 | 46.60 | 94.30 |
| HCl 3M | Blank | 4.07 | 391.24 | ---- |
| | 5 x$10^{-5}$ | 6.98 | 228.13 | 41.69 |
| | 7.5 x$10^{-5}$ | 12.08 | 131.81 | 66.30 |
| | $10^{-4}$ | 17.73 | 89.81 | 77.04 |
| | 2.5 x$10^{-4}$ | 26.36 | 60.40 | 84.55 |
| $H_2SO_4$ 0.5M | Blank | 2.58 | 246.87 | --- |
| | 5 x$10^{-5}$ | 5.71 | 176.50 | 54.81 |
| | 7.5 x$10^{-5}$ | 12.69 | 125.48 | 79.66 |
| | $10^{-4}$ | 14.18 | 112.29 | 81.80 |
| | 2.5 x$10^{-4}$ | 16.17 | 98.47 | 84.04 |
| $H_2SO_4$ 1.5M | Blank | 1.25 | 806.25 | --- |
| | 5 x$10^{-5}$ | 1.41 | 451.73 | 11.34 |
| | 7.5 x$10^{-5}$ | 2.44 | 261.04 | 48.77 |
| | $10^{-4}$ | 4.36 | 146.08 | 71.33 |
| | 2.5 x$10^{-4}$ | 9.01 | 70.69 | 86.12 |

It can be seen from table 3, that the presence of **MTI** enhances the values of $R_t$ and reduces the $C_{dl}$ values. The decrease in $C_{dl}$, which can result from a decrease in local dielectric constant and/or an increase in the thickness of the electric double layer [23], suggested that MTI molecules function by adsorption at the metal/solution interface. Thus, the decrease in $C_{dl}$ values and the increase in $R_t$ values and consequently of inhibition efficiency may be due to the gradual replacement of water molecules by the adsorption of the MTI molecules on the metal surface, decreasing the extent of dissolution reaction [24].
These impedance measurements were in good agreement with polarization tests.

**2. Adsorption isotherms**

Basic information on the interaction between the inhibitors and the mild steel surface [25] and mechanism of electrochemical reaction [26-27] may be provided by the adsorption isotherm. The surface coverage of different concentrations of inhibitor in different acidic media has been evaluated from polarization curve measurement.
Several adsorption isotherms were examined, and it was found that the adsorption of MTI in 1M HCl, 3M HCl and 0.5M $H_2SO_4$ at 298 K obeyed the Langmuir adsorption isotherm and in 1.5M $H_2SO_4$ El Awady kenetic-thermodynamic adsorption isotherm model was the most suitable model.
It can be noted that, Langmuir [28] adsorption isotherm is given by:

$$\frac{C}{\theta} = \frac{1}{K_{ads}} + C \tag{5}$$

where C is the concentration of inhibitor, Kads is the adsorption equilibrium constant and $\Theta$is the surface coverage.
And El Awady kinetic-thermodynamic adsorption isotherm [29] is defined as bellow:

$$ln\frac{\theta}{1-\theta} = \ln K' + y\, lnC \tag{6}$$

where y is the numbers of inhibitor molecules occupying one active site. If the value of y is greater than one, it implies the formation of multilayer film on the metal surface, and if the values of y are less than one, it indicates that the studied inhibitor would occupy more than one active site. K' is a constant related to the equilibrium constant of adsorption process ($K_{ads}$) by following equation:

$$K_{ads} = K'^{\left(\frac{1}{y}\right)} \tag{7}$$

From Fig. 11 it can be noted that the plots of C/Θ *vs* C (for 1M HCl, 3M HCl and 0.5M $H_2SO_4$) yielded straight lines with slope closed to one, along with linear association coefficient (R > 0.99). The kinetic –thermodynamic isotherm is presented in figure 12.

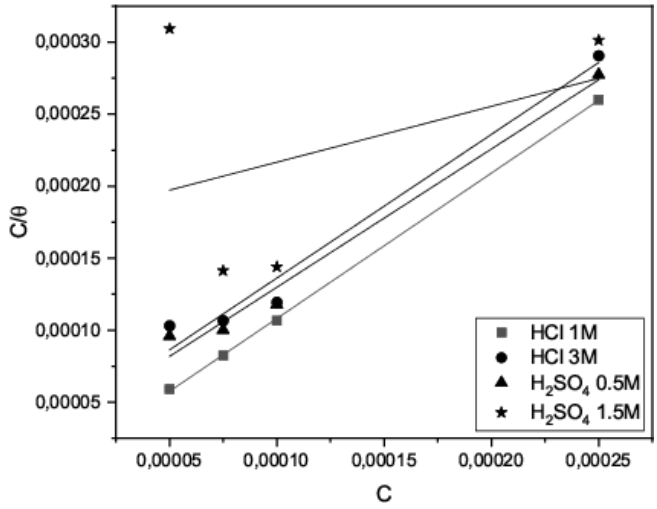


*Figure 11: Langmuir adsorption plots for mild steel in different medium in absence and presence of different concentrations of MTI at 298 K*

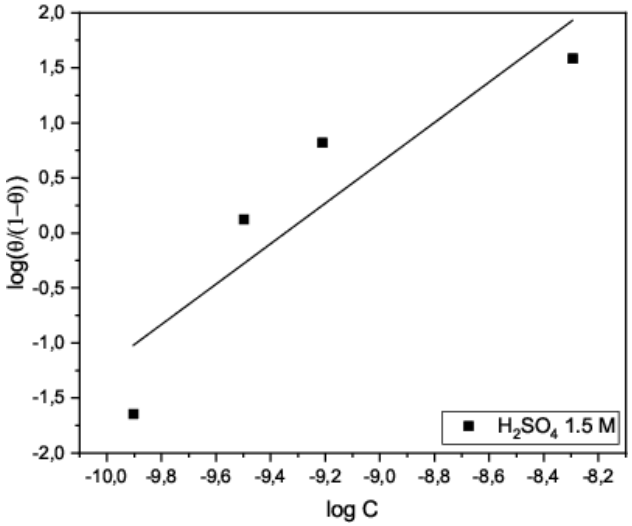


*Figure 12: El-Awady thermodynamic–kinetic model for mild steel in 1.5 M $H_2SO_4$ in absence and presence of MTI at 298 K*

In addition, the free energy of adsorption ($\Delta G_{ads}$) can be calculated according to the following equation:

$$\Delta G_{ads} = -RT \ln(55.5\ K_{ads}) \quad (8)$$

where R is the universal gas constant, T is the absolute temperature and 55.5 is the molar concentration of water in solution.

The thermodynamic parameters obtained by these adsorption isothrem are listed in table 4.

**Table 4:** Thermodynamic parameters of adsorption obtained in different medium containing MTI at 298 K

| Langmuir Isotherm | | | kinetic–thermodynamic isotherm | | |
|---|---|---|---|---|---|
| 1M HCl | K | $1.38x10^5$ | 1.5M $H_2SO_4$ | lnK' | 17.16 |
| | $\Delta G_{ads}$ | -39.27 | | y | 1,86 |
| 3M HCl | K | $2.73x10^4$ | | $K_{ads}$ | $1.01x10^4$ |
| | $\Delta G_{ads}$ | -35.26 | | $-\Delta G_{ads}$ | -32.81 |
| 0.5M $H_2SO_4$ | K | $2.95x10^4$ | | | |
| | $\Delta G_{ads}$ | -35.43 | | | |

From this table, we can see that the obtained values of 1/y is greater than one showing that a given MTI molecule occupies more than one active site.

This speculation was confirmed by the fact that the adsorption of MTI did not obey Langmuir monolayer adsorption in 1.5 M $H_2SO_4$. However, MTI in 1M HCl, 3M HCl and 0.5M $H_2SO_4$ obeyed the Langmuir isotherm and formed a single layer on the metal surface, which can be explanation for better corrosion inhibition efficiency of MTI in these medium[2-3]. From the same table, it was found that the values of $\Delta G_{ads}$ were negative, which meant the spontaneity of the adsorption process and the stability of the adsorbed layer [4].

Generally, values of $\Delta G_{ads}$ up to -20 kJ/mol are consistent with the electrostatic interaction between the charged molecules and the charged metal (physical adsorption) while those more negative than -40 kJ/mol involve sharing or transfer of electrons from the inhibitor molecules to the metal surface to form a coordinate type of bond (chemisorption) [30-31]. In the present study, the value of $\Delta G_{ads}$ is between -32 and -39 kJ/mol; probably mean that the adsorption mechanism of the MTI on mild steel in different medium is mainly the chemisorption. Noticeably, it is generally accepted that physical adsorption is preceding stage of chemisorption of inhibitors on metal surface [3].

**Explanation of adsorption and corrosion inhibition**

We can clearly see that, the inhibitor studied is more efficient in HCl medium than in $H_2SO_4$ medium, this is due to the fact that the $SO_4^{2-}$ ions are easily adsorbed and more than the $Cl^-$ ions on the metal surface therefore occupies

more active sites on the surface and leave fewer sites for organic molecules [27, 32]. On the other hand, the $Cl^-$ anion facilitates the adsorption of inhibitor cations [27, 33-34]. This explains the higher inhibitory efficacy of the inhibitor under investigation (MTI) in 1M HCl medium compared to that obtained in 0.5M $H_2SO_4$ medium. The same remark is valid for the 3M HCl medium compared to the 1.5M $H_2SO_4$ medium.

It should be noted that it is the adsorption of the inhibitory molecules at the metal / solution interface, forming a protective film which is transformed by a transition of the metal / solution interface from a state of active dissolution to the passive state. The reactive metal surface is protected from the aggressive environment by a rapid adsorption rate.

It is well recognized that organic inhibitor molecules set up their inhibition action with the adsorption of the inhibitor molecules onto the metal/solution interface. So, the adsorption process can occur through the replacement of solvent molecules from metal surface by ions and molecules accumulated in the vicinity of metal/solution interface. Ions can accumulate at the metal/solution interface in excess of those required to balance the charge on the metal at the operating potential. These ions replace solvent molecules from the metal surface and their centres reside at the inner Helmholtz plane [35-36].

The anions are adsorbed when the metal surface has an excess positive charge in an amount greater than that required to balance the charge corresponding to the applied potential. Aromatic compounds like the case of our inhibitor under investigation undergo particularly strong adsorption on many electrode surfaces. The bonding can occur between metal surface atoms and the aromatic ring of the adsorbate molecules or ligands substituent groups. The exact nature of the interactions between a metal surface and an aromatic molecule depends on the relative coordinating strength towards the given metal of the particular groups present [16]. According to the well accepted model, the adsorption of organic inhibitor molecules is often a displacement reaction involving removal of adsorbed water molecules from the metal surface [22].

In general, owing to the complex nature of adsorption and inhibition of a given inhibitor, it is impossible for single adsorption mode between inhibitor and metal surface. The adsorption of the MTI can be attributed to the presence of hetero atoms (N and S) and aromatic rings. Therefore, the possible reaction centers are unshared electron pair of heteroatoms and $\pi$-electrons of aromatic ring.

Two modes of adsorption are generally considered on the surface of metal. In one mode, the neutral **MTI** may be adsorbed on the surface of mild steel through the chemisorption mechanism, involving the displacement of water molecules from the mild steel surface and the sharing electrons between the heteroatoms and mild steel. The inhibitor molecules can also adsorb on the mild steel surface on the basis of donor–acceptor interactions between-electrons of the aromatic ring and vacant d-orbitals of surface iron atoms. In second mode, since it is well known that the steel surface bears positive charge in acid solution [3], so it is difficult for the protonated **MTI** to approach the positively charged mild steel surface ($H_3O^+$/metal interface) due to the electrostatic repulsion. Since chloride ions have a smaller degree of hydration, thus they could bring excess negative charges in the vicinity of the interface and favour more adsorption of the positively charged inhibitor molecules, the protonated **MTI** adsorb through electrostatic interactions between the positively charged molecules and the negatively charged metal surface. Thus there is a synergism between adsorbed $Cl^-$ ions and protonated **MTI** molecules. The presences of electron donating group (SH) in the aromatic ring increase the electron density on nitrogen of imidazole group, resulting high inhibition efficiency.

## Conclusions

From the overall experimental results the following conclusions can be deduced:

- The tested compound (MTI) behaves as efficient inhibitor for the acidic corrosion of mild steel.
- The corrosion inhibition efficiency increased with increasing inhibitor concentration in different medium.
- The corrosion inhibition action of the MTI is mainly due to their adsorption on the mild steel surface.
- The decrease in the corrosion rate of mild steel in the presence MTI indicated that adsorbed protective layer formed on the steel surface is persistent different medium.
- MTI was found to be mixed-type inhibitor, affecting both anodic and cathodic sites.

- Adsorption process obeyed Langmuir and El Awady kinetic-thermodynamic adsorption isotherm and regarded between physical and chemical adsorption.

**References**

[1]. Guo Y., Xu B., Liu Y., Yang W., Yin X., Chen Y., Le J., Chen Z. (2017). Corrosion inhibition properties of two imidazolium ionic liquids with hydrophilic tetrafluoroborate and hydrophobic hexafluorophosphate anions in acid medium. *J. Ind. and Eng. Chem.*, 56: 234–247.

[2]. Benikdes A., Benali O., Tidjani A., Tourabi M., Ouici H., Bentiss F. (2017). Inhibition corrosion of ductile iron by thiadiazol-thiol derivative. *J. Mater. Environm. Sci.*, 8(9): 3175-3183

[3]. Ouici H., Tourabi M., Benali O., Selles C., Jama C., Zarrouk A., Bentiss F. (2017) Adsorption and corrosion inhibition properties of 5-amino 1,3,4-thiadiazole-2-thiol on the mild steel in hydrochloric acid medium: Thermodynamic, surface and electrochemical studies. *J. Electroanal. Chem.*, 803: 125–134.

[4]. Zebida M., Benali O., Maschke U., Trainsel M. (2019) Corrosion inhibition properties of 4-methyl-2-(methylthio)-3-phenylthiazol-3-ium iodide on the carbon steel in sulfuric acid medium. *Inter. J. Corr. Scale Inhib*., 8 (3): 613-627.

[5]. Ouici H.B., Belkhouda M., Benali O., Salghi R., Bammou L., Zarrouk A., Hammouti B. (2015) Adsorption and inhibition effect of 5-phenyl-1, 2, 4-triazole-3-thione on C38 steel corrosion in 1 M HCl. *Res. Chem. Intermed.*, 41: 4617-4634.

[6]. Ouici H.B., Benali O., Guendouzi A. (2015) Corrosion Inhibition of Mild Steel in Acidic Media Using Newly Synthesized Heterocyclic Organic Molecules: Correlation between Inhibition Efficiency and Chemical Structure. *AIP Publishing*, 020086.

[7]. Bergmann I.I. (1963). *Corrosion Inhibitors*, Macemillan, New York, 126-153.

[8]. Kuznetsov Y.I. (1996) *Organic Inhibitors of Corrosion of Metals*, Springer US, 282.

[9]. Benali O., Larabi L., Traisnel M., Gengembre L., Harek Y. (2007) Electrochemical, theoretical and XPS studies of 2-mercapto-1-methylimidazole adsorption on carbon steel in 1 M $HClO_4$. *Applied Surface Science*, 253: 6130.

[10]. Jmiai A., Bourzi H., EL Ibrahimi B., EL Issami S., Bazzi L., Hilali M. (2016) Experimental and computational study of some imidazole derivatives as corrosion inhibitors for copper in sulfuric acid medium. *Inter. J. Eng. Sci. Res. Tech.*, 5(5): 235-247.

[11]. Kumar T. V., Makangara J., Laxmikanth C., Babu N. S. (2016) Computational Studies for Inhibitory Action of 2-Mercapto-1-Methylimidazole Tautomers on Steel Using of Density Functional Theory Method (DFT). *Inter. J. Comput. Theor. Chem*., 4(1): 1-6.

[12]. Milošev I., Kovacević N., Kokalj A. (2016) Effect of Mercapto and Methyl Groups on the Efficiency of Imidazole and Benzimidazole-based Inhibitors of Iron Corrosion. *Acta Chim. Slov.*, 63: 544–559

[13]. Finšgar M., Jackson J. (2014) Application of corrosion inhibitors for steels in acidic media for the oil and gas industry: A review. *Corros. Sci.*, 86: 17–41

[14]. He X., Jiang Y., Li C., Wang W., Hou B., Wu L. (2014) Inhibition properties and adsorption behavior of imidazole and 2-phenyl-2-imidazoline on AA5052 in 1.0 M HCl solution. *Corros. Sci.*, 83: 124-136.

[15]. Larabi L., Benali O., Mekelleche S. M., Harek Y. (2006) 2-Mercapto-1-methylimidazole as corrosion inhibitor for copper in hydrochloric acid, *Appl. Surf. Sci.*, 253: 1371.

[16]. Benali O., Larabi L., Tabti B., Harek Y. (2005) Influence of 1-methyl 2-mercapto imidazole on corrosion inhibition of carbon steel in 0.5 M $H_2SO_4$. *Anti-Corros. Meth. Mater.*, 52: 280

[17]. Marušić K., Ćurković H. O., Supnišek Lisac E., Takenouti H. (2018) Two Imidazole Based Corrosion Inhibitors for Protection of Bronze from Urban Atmospheres. *Croat. Chem. Acta*, 91(4): 435–446

[18]. Tsuru T., Haruyama S., Gijutsu B. (1982) Corrosion inhibition of iron by amphoteric surfactants in 2M HCl, *J. Jpn. Soc. Corros. Eng.*, 27: 573-581.

[19]. Trémillon B. (1993) *Electrochimie analytique et réactions en solution.* Edition Masson, Paris, 632.

[20]. BenHmamou D., Salghi R., Zarrouk A., Aouad M. R., Benali O., Zarrok H., Mesali M., Hammouti B., Ebenso E., Kabanda M.M, M. Bouachrine. (2013). Weight loss, electrochemical, quantum chemical calculations and molecular dynamics simulation studies on 2-(benzylthio)-1,4,5-triphenyl-1H-imidazole as inhibitor for carbon steel corrosion in hydrochloric acid, *Ind. Eng. Chem. Res.*, 52(40): 14315-14327.

[21]. Olivares-Xometl O., Álvarez-Álvarez E., Likhanova N. V., Lijanova I. V., . Hernández-Ramírez R. E, Arellanes-Lozada P., Varela-Caselis J. L. (2018). Synthesis and corrosion inhibition mechanism of ammonium-based ionic liquids on API 5L X60 steel in sulfuric acid solution, *J. Adhes. Sci. Tech.*, 32 (10): 1092-1113.

[22]. Benali O., Larabi L., Mekelleche S. M., Harek Y. (2006) Influence of substitution of phenyl group by naphthyl in a diphenylthiourea molecule on corrosion inhibition of cold-rolled steel in 0.5 M $H_2SO_4$. *J. mater. Sci.*, 41: 7064.

[23]. Boudjellal F., Ouici H.B., Guendouzi A., Benali O., Sehmi A. (2020) Experimental and theoretical approach to the corrosion inhibition of mild steel in acid medium by a newly synthesized pyrazole carbothioamide heterocycle. *Journal of Molecular Structure*, 1199: 127051.

[24]. Messikh S., Salhi R., Benali O., Ouici H. B., Gherraf N. (2020). Synthesis and evaluation of 5-(Phenyl)-4H-1,2,4-triazole-3-thiol as corrosion inhibitor for mild steel in 0.5M $H_2SO_4$ and its synergistic effect with potassium iodide. *International Journal of Chemical and Biochemical Sciences*, 17: 14-38.

[25]. Larabi L., Harek Y., Benali O., Ghalem S. (2005) Hydrazide Derivatives as Corrosion Inhibitors for Mild Steel in 1M HCl. *Prog. Org. Coat.*, 54: 256 – 262.

[26]. Jeyaprabha C., Sathiyanarayanan S., Venkatachari G. (2006) Effect of Cerium Ions on Corrosion Inhibition of PANI for Iron in 0.5 M $H_2SO_4$. *Appl. Surf. Sci.*, 253: 432 – 438.

[27]. Murthy Z.V.P., Vijayaragavan K. (2014) Mild steel corrosion inhibition by acid extract of leaves of Hibiscus sabdariffa as a green corrosion inhibitor and sorption behavior. *Green Chem. Lett. Rev.*, 7(3): 209-219.

[28]. Langmuir I. (1917). The Constitution and Fundamental Properties of Solids and Liquids. II. Liquids. *J. Am. Chem.Soc.*, 39: 1848 – 1906.

[29]. EI-Awady A.A., Abd-EI-Nabey B.A., Aziz S.G. (1992) Kinetic-Thermodynamic and Adsorption Isotherms Analyses for the Inhibition of the Acid Corrosion of Steel by Cyclic and Open-Chain Amines. *J. Electrochem. Soc.*, 139(8): 2149-2154.

[30]. Finley H.F., Hackerman N. (1960) Effect of Adsorption of Polar Organic Compounds on the Reactivity of Steel. *J. Electrochem. Soc.*, 107: 259-263.

[31]. Fouda A.S., Elewady G.Y., Shalabi K., Abd El-Aziz H.K. (2015) Alcamines as corrosion inhibitors for reinforced steel and their effect on cement based materials and mortar performance, RSC Advances, 5 (2015) 36957-36968.

[32]. M. Sivaraju, K. Kannan, V. Chandrasekaran (2005) Imidazole as a corrosion inhibitor for mild steel in acid medium. *Mater. Sci. Res. India*, 3(2): 129-134.

[33]. Hackerman N., Thompson C.D. (1973) Effect of Nitriles on the Polarization of Iron in 1.0N HCl. *Corros. Sci.*, 13: 317 – 325.

[34]. Antropov L. I. (1967) A Correlation between Kinetics of Corrosion and the Mechanism of Inhibition by Organic Compounds. *Corros. Sci.*, 7: 607 – 620.

[35]. McCafferty E., Hackerman N. (1972). Double Layer Capacitance of Iron and Corrosion inhibition with Polymethylene Diamines. *J. Electrochem. Soc.*, 119: 146.

[36]. Emregul K.C., Kurtaran R., Atakol O. (2003). An investigation of chloride-substituted Schiff bases as corrosion inhibitors for steel. *Corros. Sci.*, 45: 2803.